JTTEE5 14:224-230
DOI: 10.1361/10599630523782
1059-9630/$19.00 © ASM International

Peer Reviewed

Improvement of Corrosion Resistance of High-Velocity Oxyfuel-Sprayed Stainless Steel Coatings by Addition of Molybdenum

Jin Kawakita, Seiji Kuroda, Takeshi Fukushima, and Toshiaki Kodama

(Submitted October 6, 2003; in revised form December 3, 2003)

To improve the marine corrosion resistance of stainless steel coatings fabricated by high-velocity oxyfuel (HVOF) spraying with a gas shroud attachment, the molybdenum (Mo) content of stainless steel was increased to form coatings with a chemical composition of Fe balance-18mass%Cr-22mass%Ni-2~8mass%Mo. These coatings were highly dense, with <0.1 vol.% in porosity, and less oxidized, with 0.5 mass% in oxygen content at most. The corrosion mechanism and resistance of the coatings were investigated by electrochemical measurement, chemical analysis, and statistical processing. The general corrosion resistance of the coatings in 0.5 mol/dm^3 sulfuric acid was improved with increases in Mo content, and the corrosion rate could be decreased to 8.8 × 10^{-2} mg/cm^2 per hour (~1 mm/year) at 8 mass% Mo. The pitting corrosion resistance of the coatings in artificial seawater was improved with increases in Mo content and was superior to that of the 316L stainless steel coating. The crevice corrosion resistance of the coatings in artificial seawater was improved and the number of rust spots at 4 mass% Mo was decreased to 38% of that for the 316L coating. Accordingly, Mo is highly effective in improving the corrosion resistance of the stainless steel coatings by HVOF spraying.

Keywords corrosion resistance, gas shroud, high-velocity oxyfuel, molybdenum, stainless steel

1. Introduction

1.1 Requirements for Anticorrosion Coating

The high-velocity oxyfuel (HVOF) technique can make a dense metal coating with comparatively little change in the composition of the sprayed materials during spraying. This high performance is caused by characteristics of HVOF spraying that enable sprayed particles to have a supersonic speeds (>500 m/s) and to have lower temperatures (up to 2000 °C) compared with particles in other conventional spraying methods such as plasma spraying. The anticorrosion coatings demand an impermeable nature, above all, because any path to the substrate would allow ingress of the corrosive media to the interface between the coating and the substrate. At the interface, the electrochemically less noble steel substrate is expected to have severe corrosion damage due to the galvanic effect. Second, the intrinsic corrosion resistance of the coatings is also important because this determines the service life of coated steels if the coatings have no penetrating path. In fact, the intrinsic corrosion resistance of the HVOF-sprayed coatings is different from that of bulk plates of the same type as the coatings and depends mainly on the oxidation level of the coatings (Ref 1-3).

1.2 Past Results for Development

When the porosity is plotted against the oxygen content for a number of coatings that were prepared under various HVOF spray conditions, these two parameters show a somewhat inversely proportional relationship (Ref 3), thus indicating that it is difficult to minimize porosity and oxidation simultaneously. Therefore, a mechanism to surround the in-flight spray particles with an inert gas was developed (Ref 4, 5). Such gas-shrouding techniques have been reported (Ref 6-8). The aim was to control the oxidation of in-flight particles during thermal spraying, leading to improvement of the coating performance in corrosive environments due to a decrease in the oxidation level of the resulting coatings. The gas shroud mechanism developed in this work has a unique feature of permitting high rates of nitrogen flow over the long entrainment distance within the shroud. This mechanism can accelerate the in-flight particles, cool them, as well as prevent them from encountering oxygen in the ambient air. When American Iron and Steel Institute 316L stainless steel (SUS316L) was used as the feedstock, the average flight velocity of the sprayed particles was over 750 m/s at the substrate position, and their molten fraction was a maximum of approximately 40 mass% (Ref 5). Impingement on the target with such a high speed enables the particles to be highly deformed, leading to a dense coating with a closely packed structure. The coating formed with the gas shroud exhibited significantly low open porosity, which was less than the detection limit of mercury intrusion porosimetry (Ref 5). In addition, the low molten fraction of the in-flight particles contributes to a decrease in the oxidation level of the coating to 0.2 mass% in oxygen content. In this article, HVOF spraying with the gas shroud is termed GS-HVOF.

Coatings of the nickel-base alloy HastelloyC formed by GS-HVOF spraying, when formed on steel substrates, had zero through porosity, which resulted in no sign of substrate corrosion in artificial seawater for three months (Ref 9). In addition, the intrinsic corrosion resistance of the coatings in artificial seawater was comparable to that of a bulk plate of HastelloyC276. These coatings protected the low-carbon steel substrates, with

Jin Kawakita, Seiji Kuroda, Takeshi Fukushima, and **Toshiaki Kodama,** National Institute for Materials Science 1-2-1, Sengen, Tsukuba, Ibaraki 305-0047, Japan. Contact e-mail: kawakita.Jin@nims.go.jp.

Table 1 Spray conditions

Parameter	Unit	Value
Fuel flow rate	L/min	0.49
Oxygen flow rate	L/min	760
Combustion pressure	MPa	0.69
Fuel-oxygen ratio(a)	…	1.2
Barrel length	mm	204
Powder feed rate	g/min	60
Torch velocity	mm/s	700
Spray distance(b)	mm	380
Powder feed gas	…	Nitrogen (N_2)
Film thickness	μm	400

(a) 1.0 corresponds to the stoichiometric mixture ratio. (b) From exit of combustion chamber

Table 2 Chemical composition of feedstock powder and coating with Fe balance

	Element, mass%					
Coatings	Cr	Ni	Mo	C	O	N
Mo-2						
Powder	18.3	22.5	1.88	0.005	0.0331	<0.001
Coating	18.2	22.5	1.86	0.01	0.165	0.003
Mo-4						
Powder	18.1	22.2	3.74	0.004	0.0389	<0.001
Coating	18.1	22.1	4.13	0.012	0.301	0.004
Mo-8						
Powder	18.2	22.2	7.88	0.004	0.0417	<0.001
Coating	17.8	22.2	7.64	0.013	0.455	0.005
316L						
Powder	16.8	10.8	2.05	…	0.026	…
Coating	16.7	10.8	2.06	0.163	0.219	0.036

no corrosion damage being exhibited over 10 months in a marine exposure (Ref 3). HastelloyC is a suitable spray material because it has a high resistance against crevice corrosion in the presence of chloride. The sprayed deposits inevitably have pores and voids, which may act as a crevice to initiate corrosion; therefore, materials with a high crevice corrosion resistance are desirable (Ref 2).

1.3 Objectives of This Study

Iron-base alloys are attractive as feedstock for thermal spraying because they have the advantage of low material cost. Even with the shroud attachment, however, HVOF-sprayed coatings of SUS316L could not attain the corrosion resistance as high as the corresponding bulk plate. In fact, rust spots were observed on the surface of the 316L coating after immersion in artificial seawater for three days. The primary reason for this poor corrosion resistance was that the 316L coating is susceptible to crevice corrosion in the presence of chloride ions. To improve the crevice corrosion resistance of the stainless steel coatings, the molybdenum (Mo) content was increased. Mo is known to be an effective element for increasing the corrosion resistance of the stainless steel, especially against localized corrosion (Ref 10). The alloy composition of the coatings was assigned on the basis of the 316L composition. The nominal composition of the coatings was Fe balance-18mass%Cr-22mass%Ni-2~8mass%Mo. Nickel was also added to the 316L composition to maintain the austenite phase at 8 mass% of Mo, which is an element in the formation of the ferrite phase. The effect of Mo addition on coating properties such as oxygen content and porosity were investigated in the present work. The corrosion mechanism and resistance of the high-Mo coatings was revealed and compared with those of the 316L coating.

2. Experimental

Coatings were fabricated by HVOF spraying (JP-5000; TAFA, Concord, NH) with kerosene used as the fuel. The primary spray conditions are listed in Table 1. The feedstock powder was prepared by gas atomization under an argon atmosphere by the apparatus of Nissin Giken (Iruma, Saitama, Japan). The chemical composition of the obtained powder is listed in Table 2. The substrate material used was a nickel-base alloy so that the corrosion reaction of the coatings alone could be determined. The substrate of 5 × 50 × 100 mm was grit blasted with alumina and degreased ultrasonically in acetone prior to spraying. A pipe was attached to one end of the barrel of the HVOF gun to form the gas shroud (Ref 3-5). Nitrogen gas was injected from both ends of this pipe at flow rates of 2.5 m^3/min from upstream and at 0.45 m^3/min from downstream.

The crystalline phases of the HVOF-sprayed deposits were characterized by the x-ray diffraction (XRD) measurement using a Rigaku apparatus (RINT 2500; Rigaku, Tokyo, Japan) with Cu Kα radiation.

The cross section of the specimens was examined by optical microscopy (BX60M microscope; Olympus, Tokyo, Japan). The cross section of the specimen was prepared by embedding the specimen into an epoxy resin, part of which was removed by abrading and polishing treatments.

The chemical composition of the deposits was determined by x-ray fluorescence spectrometric analysis for metal elements, and by the inert-gas fusion method for oxygen, nitrogen, and carbon.

The open porosity was determined by mercury intrusion porosimetry (Autopore II 9220; Micromeritics, Gosford, NSW, Australia).

The corrosion mechanism and resistance of the specimen was investigated by an electrochemical polarization measurement with the three-electrode system (Ref 3). The sample electrode was prepared as follows: (a) the coated specimen was sectioned into 2.5 cm square pieces, and these were cleaned ultrasonically in acetone and ion-exchanged water; (b) the stainless steel lead was connected to the back surface of the substrate plate; and (c) a spray area of 2 cm^2 was left exposed, and the rest of the specimen surface was insulated with a silicon resin. The reference electrode was an Ag/AgCl electrode in a saturated KCl solution. The electrolyte was 0.5 mol/cm^3 sulfuric acid and artificial seawater of pH 8.3 at 300 K. The reference electrode was placed into glass tubes that were filled with the saturated KCl solution. One end of the tube was closed, and the small hole was filled with a glass filter to ensure contact of the internal solution with the electrolyte. The polarization measurement allowed the potential-current curve to be recorded by measuring the current value when the electrode potential of the sample was scanned at a rate of 10 mV/s using a potentiostat with a function generator (HAB-151; Hokuto Denko, Tokyo, Japan). The sample electrode was immersed in the electrolyte for 24 h to reach the steady

state. In this case, the counterelectrode was a platinum plate with dimensions of 0.2 × 100 × 100 mm, and continuous nitrogen bubbling was carried out for deaeration of the electrolyte. In addition, the electrode was immersed in a sulfuric acid (H_2SO_4) solution at 300 K with a concentration of 0.5 mol/dm^3.

The corrosion rate of the specimen was determined by chemical analysis of dissolution rate of the specimen immersed in the sulfuric acid. At every predetermined time, 5 mL of the test solution (0.5M H_2SO_4) was sampled, and the iron and nickel elements dissolved in the sampled solutions were determined by inductively coupled plasma (ICP) atomic emission spectrometry using an analyzer (SPS 3000; Seiko Instruments Inc., Chiba, Japan). Iron and nickel were the major elements in the deposits.

The number of rust spots observed on the surface of the specimen that was immersed in artificial seawater for 3 days were counted using photographs obtained by digital video microscope (VH-6300; KEYENCE, Osaka, Japan).

3. Results and Discussion

3.1 Physical and Chemical Properties of Coatings

The chemical composition of the coatings of high-Mo stainless steel formed by GS-HVOF spraying is listed in Table 2. All the coatings exhibited almost the same amounts of metallic elements (i.e., Cr, Ni, and Mo) as the corresponding feedstocks, indicating no remarkable occurrence of evaporation or sublimation of metallic components during the spraying process. Taking into account such a considerable similarity in terms of metallic elements, the increase in Mo content only at 4 mass% Mo may have been due to experimental error in the analytical method. On the other hand, along with an addition of Mo, there was an increase in nonmetallic elements (O, N, and C) in the coatings. This is possibly due to the strong affinity between Mo and oxygen, and the difference in the molten fraction of the in-flight spray particles, which is related to the melting point of the feedstock, depending on the Mo content. Oxygen should exist as some oxides or in the solid solution of the alloys. In the XRD pattern of the coating with 2 mass% Mo (Fig. 1a), all of the diffraction lines were assigned to the face-centered cubic (fcc) structure (i.e., the austenitic phase). In this article, the coatings with *x* mass% Mo are represented as Mo-*x* below. The peak positions of these lines were shifted to the lower angle with an increase in the Mo content (Fig. 1b and c). This arises because the lattice parameter was increased by the substitution of iron by Mo, which has a larger atomic radius, or by the solid solution of an oxygen atom into an interstitial site. As for the Mo-8 coating, additional lines attributed to the body-centered cubic structure (i.e., the ferrite phase) were observed, and the diffraction lines assigned to any oxide did not appear (Fig. 1c). The feedstock powder of Mo-8, however, consisted of the single austenite with the fcc structure. Accordingly, the formation of the ferrite phase in the Mo-8 coating was due to an excess of the content limit of Mo in the austenite phase in a part of the sprayed particles during the coating fabrication process.

The coating of high-Mo stainless steel by GS-HVOF spraying had open porosity below 0.1 vol.% under the detection limit of the instrument of mercury porosimetry. Figure 2 shows the cross-sectional images of the coatings. All of the coatings seem to have a slight number of pores or voids and ambiguous boundaries between the stacked particles. These results indicate that the high-Mo stainless steel coatings have a dense nature regardless of the Mo content up to 8 mass%.

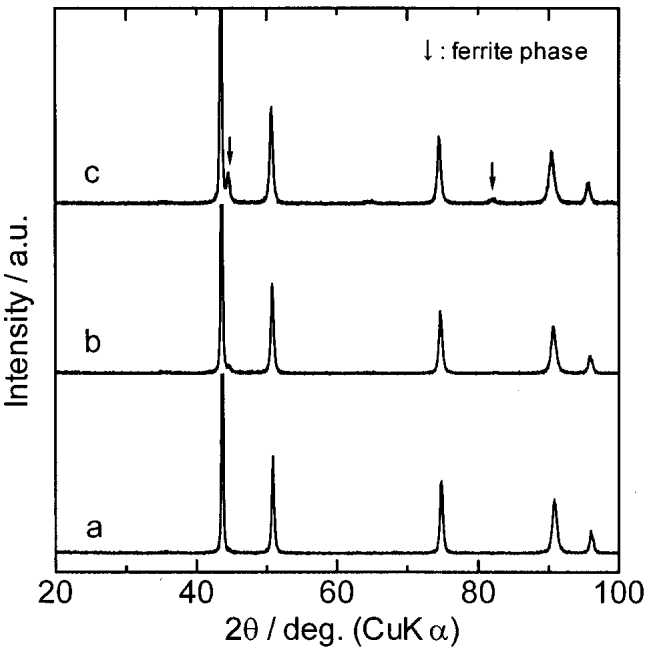

Fig. 1 XRD patterns of GS-HVOF-sprayed coatings of high-Mo stainless steel with Mo contents of (a) 2 mass%, (b) 4 mass%, and (c) 8 mass%

3.2 General Corrosion Behavior of Coatings

Figure 3 shows the anodic polarization curves of the coatings formed on the HastelloyC276 substrate in the sulfuric acid. In this research, no corrosion was considered to take place on the HastelloyC276 substrate. Even if an electrochemically less noble material such as carbon steel is used as the substrate, however, the substrate corrosion is almost negligible because the coatings are highly dense. On the polarization curves, all of the coatings, including the 316L coating, indicate the corrosion behavior that is characteristic of typical stainless steels in the sulfuric acid. The active state at a corrosion potential of approximately –250 mV was turned through the passivation region (approximately –250-400 mV) into the passive state (~400-900 mV) with the scanned electrode potential. However, all of the coatings seem to have less sharp passivation peaks and to show larger anodic currents in the passive region, compared with the bulk plate of a common stainless steel, which is typically at 10^{-6} A/cm^2. These phenomena are due to the difficulty of forming a homogeneous and dense passive film on the coatings. This is because there is some concentration gradient of oxygen between the coating surface and the inside of the pores or voids of the coatings. In addition, the surface of the sprayed particles was covered with as-formed oxides during the spraying process. The anodic current of the high-Mo stainless steel coatings was smaller than that of the 316L coating over the whole scanned electrode potential, regardless of the Mo content, particularly at 2 mass% Mo, even with the same content as at the 316L coating.

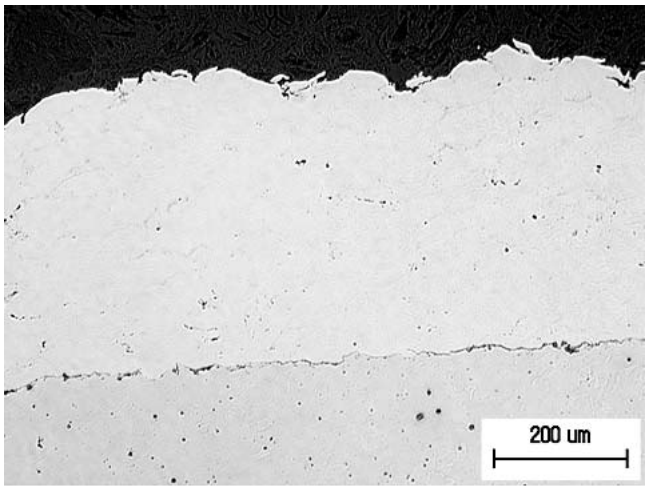

(a)

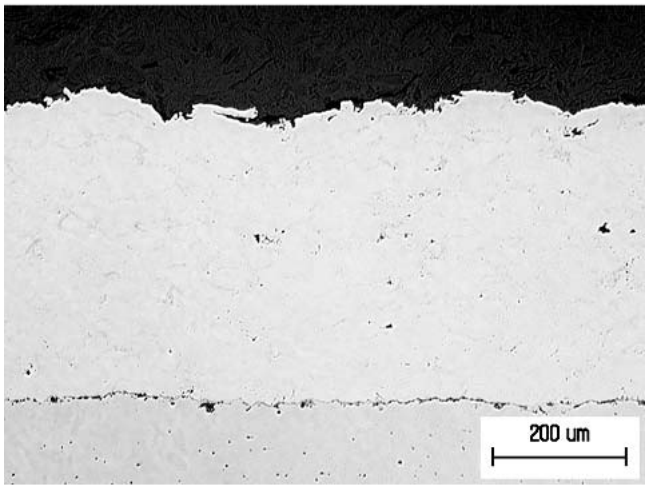

(b)

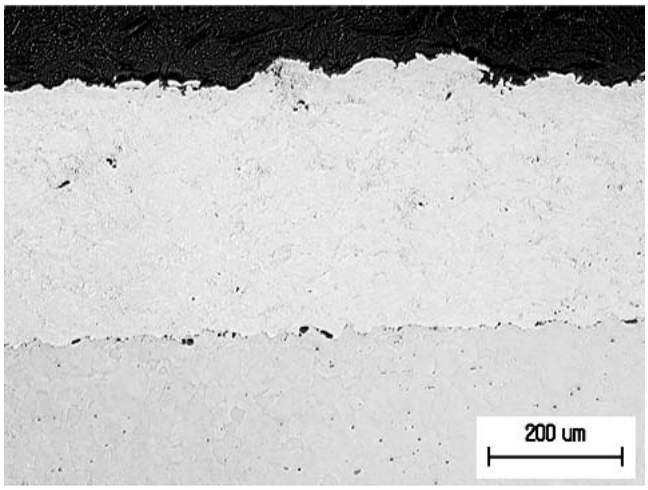

(c)

Fig. 2 Optical microscopic images of a cross section of GS-HVOF-sprayed coatings of high-Mo stainless steel with Mo contents of (a) 2 mass%, (b) 4 mass%, and (c) 8 mass%

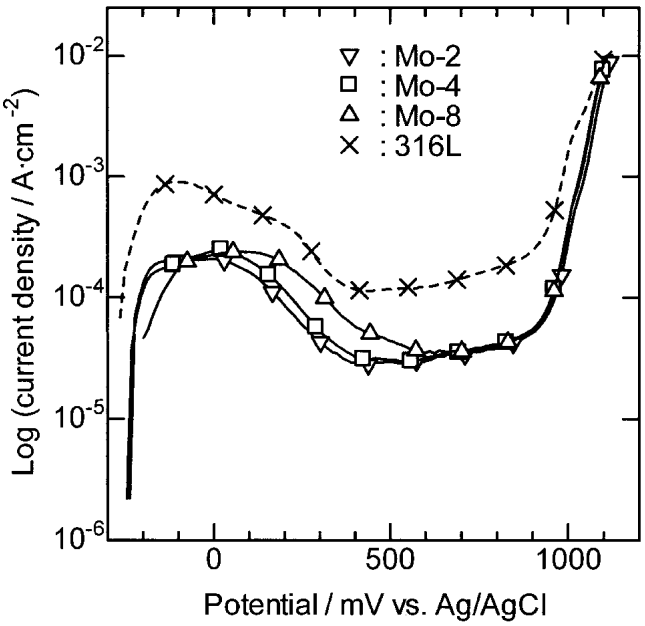

Fig. 3 Anodic polarization curves of GS-HVOF-sprayed coatings of high-Mo (Mo-*x*) and 316L stainless steel in deaerated 0.5 M sulfuric acid at 300 K. *x* is the Mo content.

This smaller anodic current, in other words, the improvement of corrosion resistance, might be due to the higher content of Ni and the lower content of C in the high-Mo stainless steel coatings, compared with those in the 316L coating (Table 2). Over 900 mV, the anodic current increases rapidly, indicating the break out of the pitting corrosion. Figure 4 shows the dependence of the dissolution rate of the coatings on the Mo content at the corrosion potential in the sulfuric acid. In this case, the corrosion of the substrate was almost negligible because the substrate was the HastelloyC276 plate. Under this condition, the coatings kept the active state, and therefore the general corrosion proceeded. In Fig. 4, the dissolution rate was calculated by dividing the dissolution rate of Fe and Ni from the coating by the content ratio of Fe and Ni in the coating, respectively. These calculations could estimate the uniform loss of the coatings (i.e., its corrosion rate), assuming that the weight loss was caused by the general corrosion. Actually, each dissolution rate that was calculated from Fe dissolution was very consistent with that from Ni dissolution. As the Mo content of the coatings increased, the resistance against general corrosion improved, and the dissolution rate of the coatings decreased to 8.8×10^{-2} mg/cm^2 per hour (~1 mm/year) at 8 mass% Mo. The coating with the Mo content >5 mass% was estimated to exceed the 316L coating in terms of corrosion resistance. Although the 316L coating has 2.0 mass% Mo at most, its coating showed a higher corrosion resistance than the coating with an Mo content up to 4 mass%. This result is different from the order of the specimens in terms of corrosion resistance estimated from the anodic current in the polarization curves (Fig. 3). This may be due to the difference in the impact of the dynamic and static corrosion states upon two types of measurements in addition to the effect of the additional elements of 316L such as N on the corrosion resistance.

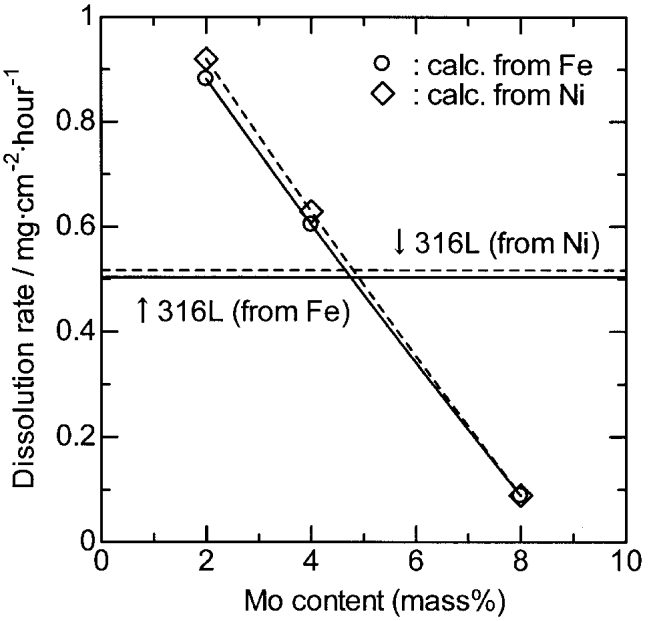

Fig. 4 Dependence of the dissolution rate of GS-HVOF-sprayed coatings of high-Mo stainless steel on Mo content in deaerated 0.5 M sulfuric acid at 300 K

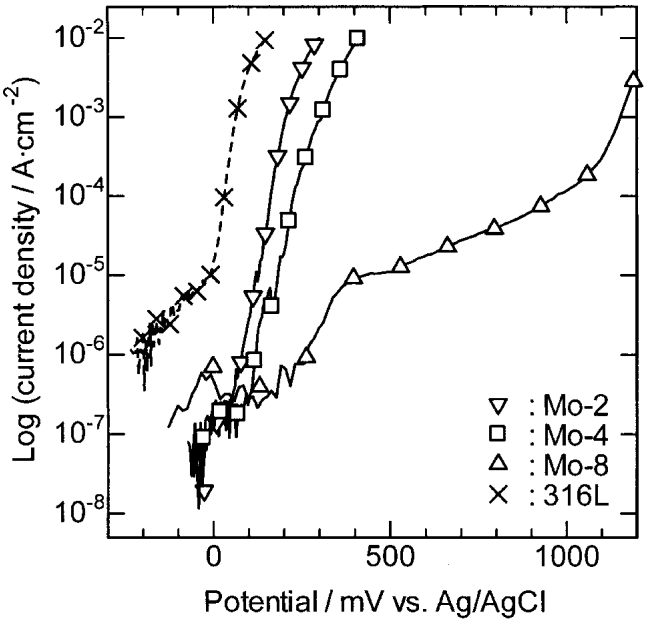

Fig. 5 Anodic polarization curves of GS-HVOF-sprayed coatings of high-Mo (Mo-*x*) and 316L stainless steel in deaerated artificial seawater at 300 K. *x* is the Mo content.

3.3 Pitting Corrosion Behavior of Coatings

Figure 5 shows the anodic polarization curves of the coatings formed on the HastelloyC276 substrate in artificial seawater. Unlike the results of the polarization measurements of the same coatings in sulfuric acid, the coatings did not show the active state at the corrosion potential as they did in the passive state. As the electrode potential of the coatings was scanned in the anodic direction, their passive state was turned into the transpassive state over the pitting potential. As for the Mo-8 coating, the anodic current increased rapidly over 200 mV, the increasing slope of the polarization curve became gentle from 400 to 1100 mV, and the anodic current increased rapidly again over 1100 mV. The former rapid increase of the anodic current and the successive gentle slope may be due to the formation of oxide, which is not so dense. In fact, the surface color of the Mo-8 coating after the polarization test was changed from gray to dull gray as a whole. A similar behavior was observed in the HastelloyC deposit by HVOF spraying (Ref 2). Figure 6 shows the dependence of the pitting potential of the coatings on the Mo content in artificial seawater. In this article, the electrode potential was defined as the pitting potential when the anodic current density reached 10 $\mu A/cm^2$ in the polarization curve. As the Mo content of the coatings increased, the pitting potential of the coatings was shifted to the noble potential, indicating that the pitting corrosion resistance had improved. The coatings with a Mo content >2.0 mass% can be estimated to exceed the corrosion resistance of the 316L coating. The improvement of the pitting corrosion resistance even at 2.0 mass% Mo content may be due to the higher Ni content of the coatings.

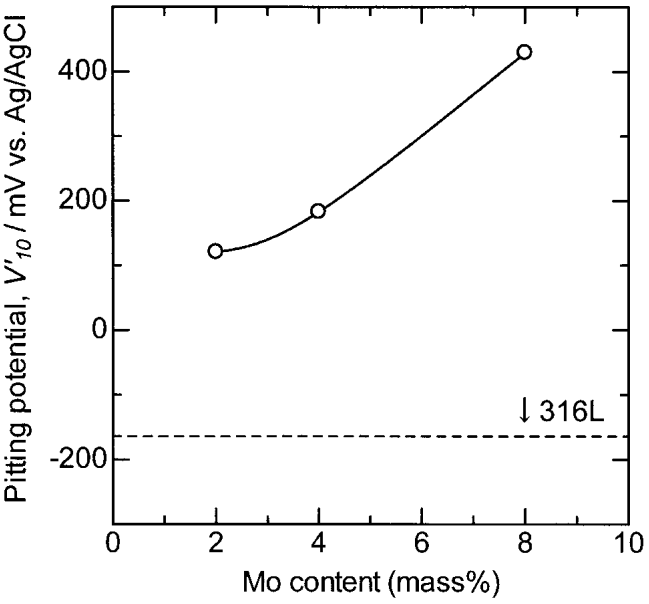

Fig. 6 Dependence of the pitting potential of GS-HVOF-sprayed coatings of high-Mo stainless steel on Mo content in deaerated artificial seawater at 300 K

3.4 Crevice Corrosion Behavior of Coatings

Figure 7 shows the appearance of the test pieces immersed in artificial seawater for three days. The inside of the circle on the test pieces was the coating formed on the HastelloyC276 substrate, and the outside was the silicon resin. The spots can be seen on the coatings' surfaces. The scanning electron microscope observation performed with microscopic elemental analysis revealed that these spots were iron oxide corresponding to the corrosion products of the coatings. Taking into account both the existence of pores or voids in the outer layer of the coatings and the passive state near the corrosion potential on the polarization

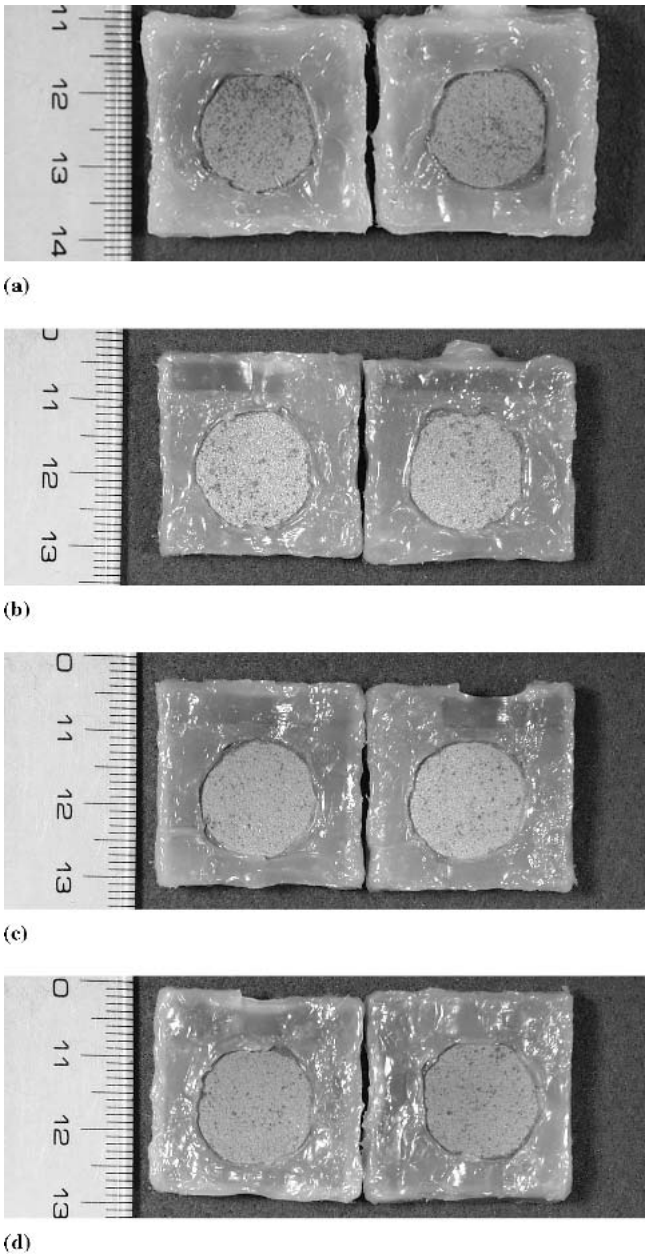

Fig. 7 Photographs of GS-HVOF-sprayed coatings of (a) 316L and high-Mo stainless steel with Mo contents of (b) 2 mass%, (c) 4 mass%, and (d) 8 mass% after immersion in aerated artificial seawater at 300 K for 3 days

curve (Fig. 5), such rust spots were considered to be caused by the crevice corrosion. The number of rust spots on the coatings was counted and compared in Fig. 8. All of the high-Mo coatings had a smaller number of rust spots than the 316L coating. The number of rust spots in the Mo-4 coating was smaller than that of the Mo-2 coating and larger than that of the Mo-8 coating. The decrease in the number of rust spots in the coating was due to the addition of Mo in the coating, and its increase at 8 mass% Mo may be due to the predominant corrosion of the ferrite phase in the coating (Fig. 2), which is expected to be less corrosion-resistant than the austenite phase. The content of the ferrite

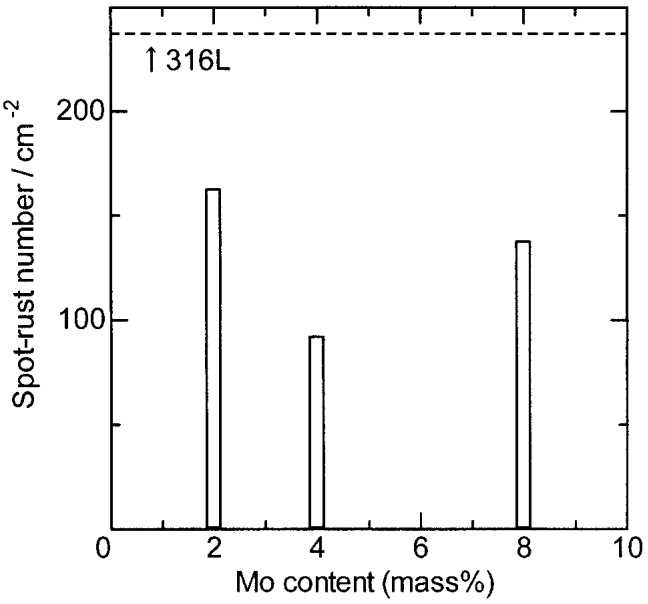

Fig. 8 Relationship between the number of rust spots and the Mo content of GS-HVOF-sprayed coatings of high-Mo stainless steel

phase is too small to contribute average or macroscopic corrosion, including general and pitting corrosion.

4. Conclusions

The coating of austenitic stainless steel with coatings of the chemical composition Fe balance-18mass%Cr-22mass%Ni-2~8mass%Mo was carried out by the GS-HVOF-spraying technique. These coatings have significantly small porosity (<0.1 vol.%) and a low oxygen content (0.46 mass%, at most).

The corrosion resistance of the coatings was improved by the addition of Mo. As a result, molybdenum was highly effective in improving the corrosion resistance of stainless steel coatings by HVOF spraying. The corrosion mechanisms were classified into three types and are summarized below.

- General corrosion resistance: the corrosion rate in sulfuric acid improved with increases in the molybdenum content. The minimum corrosion rate attained was 8.8×10^{-2} mg/cm^2 per hour (i.e., ~1 mm/year) at 8 mass% Mo.
- Pitting corrosion resistance: the pitting potential of the coatings in artificial seawater was shifted toward the noble direction with increases in the molybdenum content.
- Crevice corrosion resistance: the number of rust spots formed by crevice corrosion in artificial seawater decreased after the addition of molybdenum to the coatings. At a molybdenum content of 4 mass%, the number of rust spots became minimal and decreased to 38% of those on the 316L coating.

Acknowledgments

We are very grateful to Mr. N. Sakuma for his reliable work in preparing a number of ingots that were supplied for gas at-

omization to make feed stock powder for HVOF spraying. We greatly appreciate the experimental assistance of Mr. M. Komatsu.

References

1. J. Kawakita, T. Fukushima, S. Kuroda, and T. Kodama, Corrosion Behaviour of HVOF Sprayed SUS316L Stainless Steel in Seawater, *Corros. Sci.,* Vol 44 (No. 11), 2002, p 2561-2581
2. J. Kawakita, S. Kuroda, T. Fukushima, and T. Kodama, Corrosion Resistance of HVOF Sprayed HastelloyC Nickel Base Alloy in Seawater, *Corros. Sci.,* Vol 45 (No. 12), 2003, p 2819-2835
3. J. Kawakita, S. Kuroda, T. Fukushima, and T. Kodama, Development of Dense Corrosion Resistant Coatings By an Improved HVOF Spraying Process, *Sci. Technol. Adv. Mat. STAM.,* Vol 4 (No. 4), 2003, p 281-289
4. T. Fukushima and S. Kuroda, Oxidation of HVOF Sprayed Alloy Coatings and Its Control by A Gas Shroud, *Thermal Spray 2001: New Surfaces for A New Millennium,* C.C. Berndt, K.A. Khor, and E.F. Lugsheider, Ed., May 28-30, 2001 (Singapore), ASM International, 2001, p 527-532
5. T. Fukushima, H. Yamada, J. Kawakita, and S. Kuroda, Correlation Between the In-flight Conditions of HVOF Sprayed Alloy Particles and the Coating Structure, *International Thermal Spray Conference,* E. Lugscheider and C.C. Berndt, Ed., March 4-5, 2002 (Essen, Germany), DVS Deutscher Verband für Schweiβen, 2002, p 912-917
6. L.N. Moskowitz, Application of HVOF Spraying to Solve Corrosion Problems in the Petroleum Industry, *Thermal Spray: International Advances in Coatings Technology,* C.C. Berndt, Ed., May 25-June 5, 1992 (Orlando, FL), ASM International, 1992, p 611-618
7. V. Pershin, J. Mostaghimi, S. Chandra, and T. Coyle, A Gas Shroud Nozzle for HVOF Spray Deposition, *Thermal Spray: Meeting the Challenges of the 21st Century,* C. Coddet, Ed., May 25-29, 1998 (Nice, France), ASM International, 1998, p 1305-1308
8. C.M. Hacket and G.S. Settles, Research on HVOF Gas Shrouding for Coating Oxidation Control, *Advances in Thermal Spray Science & Technology,* C.C. Berndt and S. Sampath, Ed., Sept 11-15, 1995 (Houston, TX), ASM International, 1995, p 21-29
9. J. Kawakita, S. Kuroda, T. Fukushima, and T. Kodama, Corrosion Resistance of HastelloyC Coatings Formed by an Improved HVOF Thermal Spraying Process, *Mater. Trans. JIM.,* Vol 44 (No. 2), 2003, p 253-258
10. M. Kraack, H. Boehni, W. Muster, and J. Patscheider, Influence of Molybdenum on the Corrosion Properties of Stainless-Steel Films, *Surf. Coat. Technol.,* Vol 68, 1994, p 541-545